

1 **Cellular crosstalk between airway epithelial and endothelial cells regulates**
2 **barrier functions during exposure to double-stranded RNA**

3 **Running Head: Epithelial-endothelial crosstalk in human airways**

4 Cornelia Blume^{1*}, Riccardo Reale², Marie Held^{2,a}, Matthew Loxham¹, Timothy M.
5 Millar¹, Jane E. Collins^{1,4}, Emily J. Swindle^{1,3,4}, Hywel Morgan^{2,4}, Donna E.
6 Davies^{1,3,4}

7 ¹Academic Unit of Clinical and Experimental Sciences, Faculty of Medicine, and

8 ²Electronics and Computer Sciences, Faculty of Physical and Applied Sciences,
9 University of Southampton, Southampton, United Kingdom

10 ³National Institute for Health Research, Southampton Respiratory Biomedical
11 Research Unit, University Hospital Southampton, Southampton, United Kingdom;

12 ⁴Institute for Life Sciences, University of Southampton, Southampton, UK.

13
14 ^a current address: Department of Biochemistry, Institute for Integrative Biology,
15 University of Liverpool, Liverpool, UK

16
17 ***Corresponding author:**

18 Dr Cornelia Blume

19 Academic Unit of Clinical and Experimental Sciences, Faculty of Medicine

20 University of Southampton, University Hospital Southampton

21 Tremona Road, Southampton, SO16 6YD, UK

22 Telephone: +44 (0)2381 203390

23 Fax: +44 (0)2380 511761

24 Email: c.blume@soton.ac.uk

25

26 Abstract

27 **Introduction:** The epithelial and endothelial barriers of the airway mucosa are
28 critical for regulation of tissue homeostasis and protection against pathogens or
29 other tissue damaging agents. In response to a viral infection, epithelial cells must
30 signal to the endothelium to initiate immune cell recruitment. This is a highly
31 temporal regulated process; however, the mechanisms of this cross-talk are not fully
32 understood.

33 **Methods:** In a close-contact co-culture model of human airway epithelial and
34 endothelial cells cellular crosstalk was analysed using transepithelial electrical
35 resistance (TER) measurements, immunofluorescence, electron microscopy and
36 ELISA. Viral infections were simulated by exposing airway epithelial cells apically to
37 double-stranded RNA (Poly(I:C)). Using a microfluidic culture system the temporal
38 release of mediators was analysed in the co-culture model.

39 **Results:** Within 4h of challenge, double-stranded RNA induced the release of TNF- α
40 by epithelial cells. This activated endothelial cells by triggering the release of the
41 chemoattractant CX₃CL1 (fractalkine) by 8h post-challenge and expression of
42 adhesion molecules E-selectin and ICAM-1. These responses were significantly
43 reduced by neutralising TNF- α .

44 **Conclusion:** By facilitating kinetic profiling, the microfluidic co-culture system has
45 enabled identification of a key signalling mechanism between the epithelial and
46 endothelial barriers. Better understanding of cell-cell cross-talk and its regulatory
47 mechanisms has the potential to identify new therapeutic strategies to control airway
48 inflammation.

49

50 **Key words:** cellular crosstalk, airway epithelial barrier, endothelial barrier, Tumor
51 necrosis factor alpha, fractalkine (CX3CL1)

52 **Introduction**

53 With an estimated surface area of around 140m², the lung is the organ with the
 54 largest interface with the external environment (1). During inspiration, the lung
 55 epithelial surface is exposed to a variety of naturally occurring and anthropogenic
 56 substances with potential to do harm. However, the filtering and innate protective
 57 mechanisms of the airways inactivate and/or remove most of these substances
 58 without any need for immune cell activation (2). As well as contributing to tissue
 59 homeostasis through its barrier functions, the airway epithelium must be able to
 60 respond appropriately when it is compromised by signalling to cells of the innate and
 61 adaptive immune system (3). These immune cells may reside locally, or be recruited
 62 from the circulation via endothelial cell activation. Although the mechanisms of
 63 epithelial-endothelial crosstalk are not fully understood, communication can be
 64 achieved through release of a variety of mediators including cytokines, chemokine,
 65 growth factors, lipids and other small molecules such as reactive oxygen species
 66 (ROS) or nitric oxide (NO) (2). The integrated responses arising from this cell-cell
 67 communication can be observed readily in animal models *in vivo*, however *in vitro*
 68 models using human cells are more amenable for dissection of mechanisms of cell-
 69 cell communication and identification of key cell-type specific mediators with
 70 relevance to human disease (4).

71 Traditionally, cellular crosstalk has be analysed *in vitro* using conditioned media from
 72 one cell type to stimulate second cell type. For example, by using conditioned media
 73 from endothelial cells, it has been shown that lung endothelial cells improve the
 74 physical barrier properties of alveolar epithelial cells, while factors from brain-derived
 75 endothelial cells diminish the epithelial barrier (5). However, use of conditioned
 76 media overlooks the close spatial relationship between individual cell types within a
 77 tissue, especially direct cell-cell contacts. Crucially, it neglects the temporal evolution
 78 of mediator release. Consequently, co-culture models of different cell types have
 79 been developed to reflect the *in vivo* situation more closely. In most cases, the cell
 80 types were separated by a permeable filter support, with one cell type cultured in the
 81 apical and the other in the basolateral compartment. For example, *in vitro* models of
 82 the air-blood-barrier consisting of lung epithelial and endothelial cells have been
 83 used to study the mechanisms of acute lung injury (6). Air-blood-barrier models have
 84 also been used to analyse the passage of nanoparticles across the barrier and to

85 evaluate their immune-modulatory capacity (7-9). These improved models have led
86 to the proposal that airway epithelial-endothelial co-culture models have the potential
87 to replace *in vivo* animal studies for analysis of pulmonary toxicity (10).

88 While commonly used co-culture models represent an advance, these models lack
89 the constant exchange of metabolites or diffusion of mediators by the circulation as
90 observed *in vivo*. To address this problem, we have developed a dynamic
91 microfluidic culture system which mimics interstitial flow, enabling supply of nutrients,
92 removal of metabolites and analysis of time-dependent mediator release with much
93 higher sensitivity (11). In the current study, we have exploited this system to analyse
94 the temporal crosstalk between lung epithelial and endothelial cellular barriers in
95 response to respiratory viral infections. We hypothesised that the epithelium senses
96 the infections and activates endothelial cells to facilitate immune cell infiltration. We
97 utilised a microfluidic culture system comprising of a close-contact epithelial-
98 endothelial co-culture exposed to double stranded RNA, a virus-associated
99 molecular pattern. We found that epithelial-derived TNF- α activated endothelial cells
100 to release CX₃CL1, a chemotactic molecule for monocytes, NK cells and CD4⁺ T
101 lymphocytes (12, 13). The analysis of cellular crosstalk and the kinetics of mediator
102 release are important in order to understand the regulation of tissue homeostasis.
103 This approach provides insight into the underlying mechanisms of cellular pathology
104 in diseases including asthma and chronic obstructive pulmonary disease thereby
105 helping to identify therapeutic targets.

107 **Materials and Methods**

108 *Cell culture.* All procedures for the collection of human umbilical cords and isolation
109 of human umbilical vein endothelial cells (HUVECs) were approved by the
110 Southampton and South West Hampshire Research Ethics Committee (REC Ref:
111 07/H0502/83). HUVECs were isolated from human umbilical cords as previously
112 described (14). Briefly, the veins of umbilical cords were incubated with Type I
113 collagenase solution (1mg/ml) for 10min to remove endothelial cells. Cells in solution
114 were centrifuged and cultured on gelatin-coated tissue culture flasks in endothelial
115 culture medium (M199 medium supplemented with L-Glutamine,

penicillin/streptomycin (Life technologies, Paisley, UK) and 20% human serum) until ~80% confluent; Experiments were performed with endothelial cells in passage 1.

The human bronchial epithelial cell line, 16HBE14o- (a gift from Prof. D.C. Gruenert, San Francisco, USA), was maintained in epithelial medium (minimum essential medium (MEM) with Glutamax and supplemented with 10% foetal bovine serum and penicillin/streptomycin (Life technologies, Paisley, UK)). Cell culture flasks were coated with PureCol collagen I (Advanced BioMatrix, San Diego, CA, USA). All experiments were performed with epithelial cells for no more than 20 passages in culture.

Epithelial-endothelial co-culture. Transwell® polyester membrane cell culture inserts (6.5mm diameter, 0.4µm pore size; Corning Life Sciences, Amsterdam, The Netherlands) were used for culturing human airway epithelial and endothelial cells. Airway epithelial cells were cultured on the apical side and endothelial cells on the basal side of the permeable culture insert. After coating both sides of the membrane with collagen, inserts were turned upside-down and 5×10^4 HUVECs in a volume of 50µl endothelial medium were seeded on the basal side of the membrane. Endothelial cells were left in a humidified incubator at 37°C, 5% CO₂ for 2h to adhere. Non-adherent cells were gently washed off and the inserts replaced into a 24-well plate with 500µl endothelial medium in the basolateral compartment. Airway epithelial cells were seeded in the apical compartment at a density of 1.5×10^5 cells in 200µl epithelial cell medium. Cells were co-cultured for up to 8 days and media was changed every 2-3 days. The formation of the physical barrier was monitored by measuring the ionic permeability by transepithelial resistance (TER) using an EVOM voltohmmeter (World Precision Instruments, Aston, UK). TER measurements were corrected for the resistance of an empty Transwell (170Ω) and were expressed as Ω*cm².

Transmission Electron microscopy. Cell culture inserts were fixed with 3% glutaraldehyde and 4% paraformaldehyde in 0.1M PIPES buffer and contrast stained with 1% osmium tetroxide and 2% uranyl acetate in 0.1M PIPES buffer. After dehydration in ethanol and acetonitrile, the membranes were embedded in Spurr resin. Ultrathin sections (~60nm) were stained with Reynolds' lead citrate stain and

147 analysed with a H7000 transmission electron microscope (Hitachi High-Technologies
148 Europe GmbH, Maidenhead, UK).

149 *Immunofluorescence staining.* For immunofluorescence staining, cells were fixed in
150 4% paraformaldehyde, permeabilized with 0.1% Triton X-100 and blocked with 1%
151 BSA in PBS. Membranes were cut from the inserts and epithelial cells were stained
152 with a mouse anti-human occludin-AlexaFluor488 (clone OC-3F10, Life technologies,
153 Paisley, UK) and Acti-stain 555 phalloidin-(Cytoskeleton Inc., Denver, CO, US).
154 Endothelial cells were stained with mouse anti-human ICAM-1 and E-selectin
155 monoclonal antibodies (clone BBIG-I1 and BBIG-E1 respectively, R&D Systems,
156 Abingdon, UK) and AlexaFluor®488 conjugated goat anti-mouse IgG1 secondary
157 antibody (Life technologies, Paisley, UK). Actin filaments were stained using Acti-
158 stain 555 phalloidin. Stained membranes were mounted on slides using ProLong
159 Gold antifade reagent with DAPI (Life technologies) and analysed with a LSM6000
160 microscope (Leica Microsystems, Wetzlar, Germany). z-Stacks were deconvoluted
161 using Leica Application Suite software and z-projections and orthogonal views were
162 performed using ImageJ software.

163 *Microfluidic culture system.* The design, fabrication and validation of the microfluidic
164 culture system has been described in detail previously (11). After 6 days in co-
165 culture, cells on inserts were transferred to microfluidic culture device and perfused
166 with endothelial medium at a flow rate of 30µl/h (Fig. 1). Following an equilibration
167 phase of 1h, epithelial cells were apically exposed to 5µg/ml Poly(I:C) (HMW, 1.5kb
168 to 8kb, Invivogen, Toulouse, France) to mimic a viral infection. Basolateral secretions
169 were collected with an automated fraction collector every 2h for a period of 24h.
170 Control experiments were performed under static culture conditions in 24-well plates
171 with 200µl apical and 500µl basolateral medium.

172 *Release of mediators.* The release of TNF-α and CX₃CL1 (fractalkine) into the
173 basolateral medium was analysed by ELISA using Human TNF-alpha DuoSet and
174 Human CX₃CL1/Fractalkine DuoSet kits (R&D Systems, Abingdon, UK). For blocking
175 experiments, the soluble TNF-α receptor fusion protein, Enbrel (Wyeth Europa Ltd,
176 Maidenhead, UK) was added to the apical and basolateral medium at a
177 concentration of 10µg/ml, 1h prior stimulation.

Macromolecular permeability. FITC-labelled dextran with an average molecular weight of 4kDa was added to the apical medium at a concentration of 2mg/ml for the last 3h of stimulation. The amount of FITC-dextran passage to the basolateral compartment was analysed by measuring the fluorescence intensity and taken as a measure of macromolecular permeability.

Statistical analysis. Statistical evaluation was performed using the software SigmaPlot 12.5. If not stated otherwise, related samples were analysed for statistical significance using the non-parametric Wilcoxon test. Differences were regarded as significant when $P \leq 0.05$.

Results

Improved physical barrier in co-culture. The barrier properties of the co-culture model were monitored by transepithelial resistance (TER), a measure of the ionic permeability. As shown in Figure 2A, the TER in the co-cultures was significantly increased from day 1 of culture compared to epithelial mono-cultures. At day 3 of culture, a maximum was reached with the co-cultures showing more than a 2-fold increase in TER compared with epithelial mono-cultures. Over the following days the TER was slightly reduced in the co-cultures, but remained around 2-fold higher than the epithelial mono-cultures. The close proximity of the epithelial and endothelial cells in the co-culture model was important for the observed decrease in ionic permeability in the co-cultures, since culturing the endothelial cells at the bottom of the culture plate rather than directly on the basolateral side of the permeable filter support resulted in a smaller increase in TER (Figure 2B). Furthermore, soluble factors released by endothelial cells triggered the increase in epithelial TER, since conditioned media from endothelial cells caused a 1.5-fold increase in TER (Figure 2C). However, this increase caused by conditioned media was lower than the increase in TER observed in the co-culture model again confirming the importance of the close proximity of the two cell types.

Morphology of co-cultures. Epithelial and endothelial cells were cultured together in close proximity for a period in which the polarisation of the epithelial layer occurred. After 6-8 days in culture, immunofluorescence microscopy showed that epithelial

cells in either mono- or co-culture had zonular apicolateral staining at cell-cell contacts with antibodies specific for the tight junction protein, occludin, with F-actin showing a broadly similar organization (Figure 3A-D). However, in the co-cultures the occludin was more regularly organised at the subapical lateral regions of the cells (Figure 3E and F) and the thickness of the epithelial cell sheet ($10.82\mu\text{m} \pm 0.83$ mean \pm SD) was significantly reduced compared with monocultures ($21.15\mu\text{m} \pm 3.34$ mean \pm SD; $p=0.0214$; paired t-test). Electron microscopy confirmed that the epithelial cells in the co-cultures had formed a more even cell sheet with a pseudostratified structure whereas the epithelial monocultures showed little evidence of stratification and the apical surface was more irregular (Figure 3G and H).

Effect of Poly(I:C) on physical barrier. As previously reported (15), apical exposure of polarised epithelial monocultures to double-stranded RNA (Poly(I:C)), a virus-associated molecular pattern that mimics viral infections, caused a reduction in the TER as early as 3h after exposure (Figure 4A). The minimum occurred 6h after exposure with a level that was around 50% lower than the untreated control, and there was a slight recovery by 24h after exposure. In the co-culture, a similar response to Poly(I:C) was detected with a drop in TER 3h after exposure and a 50% decrease compared with the untreated control. However, the absolute TER value of the co-cultures with Poly(I:C) treatment remained higher and was at the same level of the untreated epithelial monoculture. Both epithelial mono-cultures and epithelial-endothelial co-cultures showed a dose-dependent reduction in TER after stimulation with Poly(I:C) for 24h (Figure 4B). Although Poly(I:C) caused a significant increase in ionic permeability, this was associated with only small increases in macromolecular permeability as determined by passage of FITC-dextran (Figure 4C), but again the overall permeability of the co-cultures was lower and was similar to the untreated epithelial monoculture. In contrast to cultures containing epithelial cells, the endothelial cell monocultures had comparatively low TER values ($25\Omega\cdot\text{cm}^2$) compared to epithelial cells ($564.7\Omega\cdot\text{cm}^2 \pm 72.6$ SEM) and epithelial-endothelial co-cultures ($1053.9\Omega\cdot\text{cm}^2 \pm 104.7$ SEM). Additionally, endothelial cells exhibited 40-50 times higher macromolecular permeability, suggesting that the epithelial cells contributed most to the tight barrier properties of the co-culture.

Using static culture conditions, we analysed mediator release in response to Poly(I:C) challenge (Suppl. Figure 1). TNF- α release was significantly increased by Poly(I:C) in epithelial monocultures and co-cultures, while endothelial monocultures released very low levels of TNF- α which were reduced after Poly(I:C) treatment (Suppl. Figure 1A). Poly(I:C) not only stimulated release of CX₃CL1 in the co-culture (Suppl. Figure 1B), but also directly stimulated CX₃CL1 release from endothelial cells. Interestingly, the baseline levels of released CX₃CL1 were increased in the co-culture, an effect that might be caused by soluble factors released by epithelial cells. Taken together, our data suggested that Poly(I:C) drives epithelial release of TNF- α and endothelial release of CX₃CL1.

Kinetic of mediator release. Using a microfluidic culture system (Figure 1), we were able to analyse the kinetics of mediator release in co-cultures and epithelial monocultures. As shown in Figure 5A, Poly(I:C) induced release of TNF- α which peaked as early as 4h and was reduced to background level 8h after stimulation. The kinetics of TNF- α release was comparable in epithelial monocultures and co-cultures, however, consistent with the static culture system, release of TNF- α in the co-culture was slightly lower than in epithelial monocultures. This might be explained by utilization of TNF- α binding to receptors present on endothelial cells. Similar to the static cultures, CX₃CL1 release was only detected in the co-cultures and not in epithelial monocultures, suggesting that the CX₃CL1 release is derived from the endothelial cells (Figure 5B). In the co-cultures, maximal CX₃CL1 release occurred 8h after stimulation and returned to baseline level by 18h.

Regulation of endothelial CX₃CL1 release. Although Poly(I:C) was able to directly stimulate CX₃CL1 release by endothelial cells, the changes in macromolecular permeability of the epithelial-endothelial cell co-cultures were low, suggesting that little Poly(I:C) would penetrate across the epithelial barrier and come into direct contact with the endothelial cells. However, the timing of cytokine release detected using the microfluidic culture system suggested that the epithelial-derived TNF- α observed 4h after stimulation might trigger endothelial CX₃CL1 release observed 8h after stimulation. To test this hypothesis, we used Etanercept, a soluble TNF- α receptor to antagonize the effect of TNF- α . This caused a significant reduction of CX₃CL1 release by the co-cultures after Poly(I:C) stimulation (Figure 6), indicating

that cellular cross talk is occurring with epithelial derived TNF- α driving the release of endothelial CX₃CL1, rather than the Poly(I:C) directly stimulating the endothelial cells. In contrast, blocking TNF- α did not alter the Poly(I:C)-induced effect on TER (Suppl. Figure 2A+B).

Expression of endothelial adhesion molecules. After Poly(I:C) stimulation, the expression of endothelial adhesion molecules in epithelial-endothelial co-cultures was analysed by fluorescence microscopy. As shown in Figure 7, the endothelial cells showed an increased expression of the adhesion molecules, ICAM-1 and E-selectin after Poly(I:C) stimulation of the co-cultures. This increase in expression was reduced by neutralizing TNF- α , indicating that epithelial-derived TNF- α also triggered the expression of endothelial adhesion molecules in response to double-stranded RNA.

Discussion

In this study, we demonstrated that cellular crosstalk plays an important role in coordinating barrier functions of the airway epithelium and endothelium. Through use of a close contact co-culture model, we showed that the epithelial barrier properties are enhanced, an effect that is mediated by the presence of endothelial-derived mediators. In conjunction, we observed morphological changes of the epithelium suggesting that endothelial cells support the maturation of the epithelium into a pseudostratified layer, although complete differentiation into a mucociliary epithelium was not observed. Furthermore, in response to double-stranded RNA (Poly(I:C)), the epithelium responds rapidly and transiently by releasing TNF- α which activates endothelial cells to produce CX₃CL1 and express adhesion molecules. This coordinated response is important in regulating immune cell transmigration across the endothelial barrier and into the tissue. While microfluidic models of the alveolar-capillary interface have been developed (16, 17), our microfluidic culture model of the airways allowed us to analyse for the first time the temporal release of these mediators in response to double-stranded RNA and to show that TNF- α release by epithelial cells is preceded by, and required for, CX₃CL1 release by endothelial cells. A key advantage of our microfluidic culture system over conventional static culture is

that it simulates interstitial flow and limits accumulation of mediators, as occurs in vivo. Thus, it allows for temporal control of mediator release to be analysed in great detail, at shorter time intervals, and with a higher sensitivity. This will allow detailed investigations of the primary or up-stream regulatory mechanisms that control cellular crosstalk and help to identify key processes that are dysfunctional in diseases, especially inflammatory chronic lung diseases like asthma and chronic obstructive pulmonary disease (COPD). Furthermore, this complex dynamic human 3D *in vitro* model has the potential to reduce and replace animal experiments for analysing pathological mechanisms underlying chronic lung diseases, as animal models have only limited transferability into the human disease (18).

Improvement of the physical barrier properties during lung epithelial-endothelial co-cultures has been shown previously. For example, Chowdhury et al. (19) reported improved physical barrier properties measured by TER in an airway epithelial-endothelial co-culture model, an effect that was mediated by endothelial derived factors. However, they did not observe morphological changes in the airway epithelium in the co-cultures. This might be due to a difference in the co-culture model, since the endothelial cells were introduced after completion of epithelial polarisation while in the current study, epithelial and endothelial cells were co-cultured during the period of epithelial polarisation. Interestingly, this barrier improving effect of endothelial cells seems to be tissue specific, since endothelial cells derived from brain tissue have been reported to cause a weakening of the physical barrier of lung epithelial cells (5). Reduced barrier properties have also been reported in retinal epithelial and endothelial co-cultures (20). The endothelial-derived factors mediating the enhancing or reducing effects on the epithelial barrier and the mechanisms are still unknown.

Poly(I:C), an analogue of double-stranded RNA that mimics viral replication, has been evaluated for its effects on airway barrier functions previously. Airway epithelial cells express various pattern-recognition receptors (PRRs) to sense double-stranded RNA, including toll-like receptor 3 (TLR3), protein kinase D (PKD) and cytoplasmic helicases like RIG-I and MDA5 (15, 21). Similar to our data, increased ionic permeability has been detected within the first 3h after exposure of polarised 16HBE14o- cells to Poly(I:C) and this was linked to an increase in macromolecular permeability (15). The decrease in physical barrier integrity has been associated with

disassembly of adherens and tight junction proteins, a process that is thought to be mediated by PKD (15). However, although Poly(I:C) increased the ionic permeability of the co-culture, the effect on macromolecular permeability was small and the permeability was similar to that of untreated epithelial monocultures which exhibit good barrier properties and low macromolecular permeability. Consequently, it seemed unlikely that apically applied Poly(I:C) would be able to penetrate the epithelial barrier to directly activate the underlying endothelial cells.

Double-stranded RNA is also able to induce the release of inflammatory mediators by airway epithelial cells, which include the release of CXCL8/IL-8, CXCL10/IP-10, IFN- β and TNF- α (22). Here we show that double-stranded RNA induced the release of TNF- α by airway epithelial cells. TNF- α is an important inflammatory mediator that acts on many cell types including fibroblasts, endothelial cells and immune cells as well as epithelial cells themselves. For example, exposure of differentiated bronchial epithelial cells to TNF- α over 4 days resulted in an increased ionic and macromolecular permeability of the barrier and stimulated release of cytokines and metalloproteases (23). TNF- α is also thought to trigger mucus production in airway epithelial cells (24). However, *in vivo*, release of mediators shows a time-dependency that facilitates cellular crosstalk in response to environmental impacts. Using a dynamic microfluidic *in vitro* culture system that simulates interstitial flow, we have been able to analyse the kinetics of the mediator release with a higher sensitivity and accuracy compared to conventional static culture conditions (11). By using this dynamic culture system in combination with the epithelial-endothelial co-culture model, we were able to show that epithelial cells release TNF- α rapidly after challenge with Poly(I:C), peaking 4 hours after exposure and falling to basal levels by 10-12 hours. Although we showed that endothelial cells can respond to direct stimulation by Poly(I:C), in the co-culture system with both epithelial and endothelial barriers acting in a co-ordinated fashion, early release of TNF- α by airway epithelial cells was shown to be responsible for endothelial cell release of CX₃CL1. Epithelial-derived TNF- α also induced the expression of the adhesion molecules ICAM-1 and E-selectin.

TNF- α is a well-known regulator of endothelial functions and its mechanisms were studied extensively (25, 26). Using endothelial monocultures, induction of CX₃CL1

after stimulation with exogenous TNF- α has been shown previously (27, 28). By facilitating kinetic profiling, the microfluidic co-culture system has enabled identification of TNF- α as a key endogenous signalling mechanism between the epithelial and endothelial barriers. It is thought that TNF- α induces the transcription of CX₃CL1 by a phosphatidylinositol 3'-kinase and NF- κ B mediated pathway (27). Additionally, TNF- α has been shown to stabilise CX₃CL1 mRNA via a p38 MAPK dependent mechanism on a post-transcriptional level, which results in synergistically induced CX₃CL1 expression in HUVECs after TNF- α and IFN- γ stimulation (28). Released soluble CX₃CL1 is involved in leukocyte trafficking by attracting and activating CD8⁺ and CD4⁺ T cells, natural killer cells, dendritic cells and monocytes (29). There is evidence that CX₃CL1 is linked to inflammatory chronic lung diseases as raised levels of CX₃CL1 have been shown in asthma and COPD (30, 31).

Activation of endothelial cells by TNF- α also results in the expression of adhesion molecules facilitating the transmigration of leukocytes across the endothelial barrier. For example, TNF- α is a well-known inducer of endothelial adhesion molecule expression like E-selectin and ICAM-1 which is mediated by the NF- κ B and AP-1 signalling pathways (25, 26). Recent data showed that the expression of E-selectin is induced by TNF- α by a p66^{S_{hc}} and JNK-mediated pathway and results in increased transmigration of leukocytes (32). Since blockade of TNF- α only partially prevents endothelial activation, other epithelial-derived factors, such as IL-8 or IFN- β , may contribute to endothelial activation. IL-8 has been shown to initiate the reorganisation of the endothelial cytoskeleton (33) and IFN- β modulates endothelial expression of ICAM-1 and MHC class I and II molecules (34).

After endothelial activation the recruitment of immune cells is mediated by a highly regulated adhesion cascade including the capture, rolling, crawling and finally the transmigration of the immune cell across the endothelial barrier, a process that has been intensively studied (35, 36). Since TNF- α plays a central role in the regulation of inflammation, TNF-blocking biologicals are already approved for the treatment of inflammatory diseases including rheumatoid arthritis, inflammatory bowel disease and psoriasis (37, 38). The efficacy of anti-TNF- α drugs in pulmonary inflammatory diseases such as asthma has been investigated (39-41), as well as the use of other non-biological drugs like polyphenols (42). However, the role of TNF- α mediated

endothelial activation in virally induced lung inflammation is less well characterised. Since viral infections are the most common trigger of exacerbations in chronic lung diseases like asthma and COPD, targeting adhesion molecules involved in immune cell recruitment is a promising therapeutic strategy (43). Using an epithelial-endothelial co-culture model in combination with a dynamic culture platform allows us to identify a key signalling mechanism between the epithelial and endothelial barriers. This should enhance our understanding of the regulatory mechanisms during airway inflammation and contribute to the identification of new, more effective drugs targeting chronic airway inflammation. Additionally, the dynamic co-culture model of the airway mucosa is an ideal tool for testing candidate drugs for their efficacy in the pre-clinical phase, since it incorporates the aspect of cellular crosstalk and the dynamic flow of metabolites observed *in vivo*.

Limitations of the study. The aim of this study was to highlight the potential for utilisation of microfluidic culture systems with epithelial-endothelial co-culture models to enable kinetic analysis of the mediators involved in cell-cell communication between the epithelial and endothelial barriers. In order to facilitate uptake of the model by the scientific community and to ensure accessibility to human cell material, we utilised an airway epithelial cell line (16HBE) that forms a polarised barrier in culture and human umbilical cord endothelial cells (HUVECs). Both cell types have been used extensively to study airway epithelial and endothelial functions. For example, we and others have found that 16HBE cells and fully differentiated primary bronchial epithelial cells respond similar to challenge with pollen (44) or Poly(I:C) (45). However, in future work it will be important to evaluate the co-culture model using fully differentiated primary bronchial epithelial cells and pulmonary (or bronchial) microvascular endothelial cells. Furthermore, while we elected to use Poly(I:C) as a proto-typical pathogen-associated molecular pattern (PAMP) that mimics the production of double-stranded RNA during viral replication, this only reflects one aspect of viral infection. In order to reflect the complexity of human rhinovirus infections, further work would be required using infectious respiratory viruses.

References

1. Gehr P, Bachofen M, Weibel ER. The normal human lung: ultrastructure and morphometric estimation of diffusion capacity. *Respiration physiology*. 1978;32(2):121-40. Epub 1978/02/01.

2. Loxham M, Davies DE, Blume C. Epithelial Function and Dysfunction in Asthma. *Clinical and experimental allergy : journal of the British Society for Allergy and Clinical Immunology*. 2014. Epub 2014/03/26.

3. Davies DE. Epithelial barrier function and immunity in asthma. *Annals of the American Thoracic Society*. 2014;11 Suppl 5:S244-51. Epub 2014/12/20.

4. Blume C, Davies DE. In vitro and ex vivo models of human asthma. *European journal of pharmaceuticals and biopharmaceuticals : official journal of Arbeitsgemeinschaft fur Pharmazeutische Verfahrenstechnik eV*. 2013;84(2):394-400. Epub 2013/01/15.

5. Neuhaus W, Samwer F, Kunzmann S, Muellenbach RM, Wirth M, Speer CP, et al. Lung endothelial cells strengthen, but brain endothelial cells weaken barrier properties of a human alveolar epithelium cell culture model. *Differentiation; research in biological diversity*. 2012;84(4):294-304. Epub 2012/10/02.

6. Wang L, Taneja R, Wang W, Yao LJ, Veldhuizen RA, Gill SE, et al. Human alveolar epithelial cells attenuate pulmonary microvascular endothelial cell permeability under septic conditions. *PloS one*. 2013;8(2):e55311. Epub 2013/02/09.

- 451 7. Bengalli R, Mantecca P, Camatini M, Gualtieri M. Effect of nanoparticles and
452 environmental particles on a cocultures model of the air-blood barrier. *BioMed*
453 *research international*. 2013;2013:801214. Epub 2013/03/20.
- 454 8. Kasper J, Hermanns MI, Bantz C, Maskos M, Stauber R, Pohl C, et al.
455 Inflammatory and cytotoxic responses of an alveolar-capillary coculture model to
456 silica nanoparticles: comparison with conventional monocultures. *Particle and fibre*
457 *toxicology*. 2011;8(1):6. Epub 2011/01/29.
- 458 9. Sisler JD, Pirela SV, Friend S, Farcas M, Schwegler-Berry D, Shvedova A, et
459 al. Small airway epithelial cells exposure to printer-emitted engineered nanoparticles
460 induces cellular effects on human microvascular endothelial cells in an alveolar-
461 capillary co-culture model. *Nanotoxicology*. 2014:1-11. Epub 2014/11/12.
- 462 10. Snyder-Talkington BN, Schwegler-Berry D, Castranova V, Qian Y, Guo NL.
463 Multi-walled carbon nanotubes induce human microvascular endothelial cellular
464 effects in an alveolar-capillary co-culture with small airway epithelial cells. *Particle*
465 *and fibre toxicology*. 2013;10:35. Epub 2013/08/02.
- 466 11. Blume C, Reale R, Held M, Millar TM, Collins JE, Davies DE, et al. Temporal
467 Monitoring of Differentiated Human Airway Epithelial Cells Using Microfluidics. *PLoS*
468 *one*. 2015;10(10):e0139872. Epub 2015/10/06.
- 469 12. Julia V. CX3CL1 in allergic diseases: not just a chemotactic molecule. *Allergy*.
470 2012;67(9):1106-10. Epub 2012/07/07.

- 471 13. White GE, Greaves DR. Fractalkine: a survivor's guide: chemokines as
472 antiapoptotic mediators. *Arteriosclerosis, thrombosis, and vascular biology*.
473 2012;32(3):589-94. Epub 2012/01/17.
- 474 14. Bartczak D, Muskens OL, Sanchez-Elsner T, Kanaras AG, Millar TM.
475 Manipulation of in vitro angiogenesis using peptide-coated gold nanoparticles. *ACS*
476 *nano*. 2013;7(6):5628-36. Epub 2013/05/30.
- 477 15. Rezaee F, Meednu N, Emo JA, Saatian B, Chapman TJ, Naydenov NG, et al.
478 Polyinosinic:polycytidylic acid induces protein kinase D-dependent disassembly of
479 apical junctions and barrier dysfunction in airway epithelial cells. *The Journal of*
480 *allergy and clinical immunology*. 2011;128(6):1216-24 e11. Epub 2011/10/15.
- 481 16. Huh D, Matthews BD, Mammoto A, Montoya-Zavala M, Hsin HY, Ingber DE.
482 Reconstituting organ-level lung functions on a chip. *Science*. 2010;328(5986):1662-8.
483 Epub 2010/06/26.
- 484 17. Huh D, Leslie DC, Matthews BD, Fraser JP, Jurek S, Hamilton GA, et al. A
485 human disease model of drug toxicity-induced pulmonary edema in a lung-on-a-chip
486 microdevice. *Science translational medicine*. 2012;4(159):159ra47. Epub 2012/11/09.
- 487 18. Holmes AM, Solari R, Holgate ST. Animal models of asthma: value, limitations
488 and opportunities for alternative approaches. *Drug discovery today*. 2011;16(15-
489 16):659-70. Epub 2011/07/05.
- 490 19. Chowdhury F, Howat WJ, Phillips GJ, Lackie PM. Interactions between
491 endothelial cells and epithelial cells in a combined cell model of airway mucosa:

- 492 effects on tight junction permeability. *Experimental lung research*. 2010;36(1):1-11.
493 Epub 2010/02/05.
- 494 20. Hartnett ME, Lappas A, Darland D, McColm JR, Lovejoy S, D'Amore PA.
495 Retinal pigment epithelium and endothelial cell interaction causes retinal pigment
496 epithelial barrier dysfunction via a soluble VEGF-dependent mechanism.
497 *Experimental eye research*. 2003;77(5):593-9. Epub 2003/10/11.
- 498 21. Wang Q, Nagarkar DR, Bowman ER, Schneider D, Gosangi B, Lei J, et al.
499 Role of double-stranded RNA pattern recognition receptors in rhinovirus-induced
500 airway epithelial cell responses. *J Immunol*. 2009;183(11):6989-97. Epub 2009/11/06.
- 501 22. Ritter M, Mennerich D, Weith A, Seither P. Characterization of Toll-like
502 receptors in primary lung epithelial cells: strong impact of the TLR3 ligand poly(I:C)
503 on the regulation of Toll-like receptors, adaptor proteins and inflammatory response.
504 *J Inflamm (Lond)*. 2005;2:16. Epub 2005/12/01.
- 505 23. Hardyman MA, Wilkinson E, Martin E, Jayasekera NP, Blume C, Swindle EJ,
506 et al. TNF-alpha-mediated bronchial barrier disruption and regulation by src-family
507 kinase activation. *The Journal of allergy and clinical immunology*. 2013;132(3):665-
508 75 e8. Epub 2013/05/02.
- 509 24. Lora JM, Zhang DM, Liao SM, Burwell T, King AM, Barker PA, et al. Tumor
510 necrosis factor-alpha triggers mucus production in airway epithelium through an
511 IkappaB kinase beta-dependent mechanism. *The Journal of biological chemistry*.
512 2005;280(43):36510-7. Epub 2005/08/27.

- 513 25. Poher JS. Endothelial activation: intracellular signaling pathways. Arthritis
514 research. 2002;4 Suppl 3:S109-16. Epub 2002/07/12.
- 515 26. Marcos-Ramiro B, Garcia-Weber D, Millan J. TNF-induced endothelial barrier
516 disruption: beyond actin and Rho. Thrombosis and haemostasis. 2014;112(6):1088-
517 102. Epub 2014/08/01.
- 518 27. Ahn SY, Cho CH, Park KG, Lee HJ, Lee S, Park SK, et al. Tumor necrosis
519 factor-alpha induces fractalkine expression preferentially in arterial endothelial cells
520 and mithramycin A suppresses TNF-alpha-induced fractalkine expression. The
521 American journal of pathology. 2004;164(5):1663-72. Epub 2004/04/28.
- 522 28. Matsumiya T, Ota K, Imaizumi T, Yoshida H, Kimura H, Satoh K.
523 Characterization of synergistic induction of CX3CL1/fractalkine by TNF-alpha and
524 IFN-gamma in vascular endothelial cells: an essential role for TNF-alpha in post-
525 transcriptional regulation of CX3CL1. J Immunol. 2010;184(8):4205-14. Epub
526 2010/03/17.
- 527 29. Zhang J, Patel JM. Role of the CX3CL1-CX3CR1 axis in chronic inflammatory
528 lung diseases. International journal of clinical and experimental medicine.
529 2010;3(3):233-44. Epub 2010/09/10.
- 530 30. Rimaniol AC, Till SJ, Garcia G, Capel F, Godot V, Balabanian K, et al. The
531 CX3C chemokine fractalkine in allergic asthma and rhinitis. The Journal of allergy
532 and clinical immunology. 2003;112(6):1139-46. Epub 2003/12/06.

- 533 31. Ning W, Li CJ, Kaminski N, Feghali-Bostwick CA, Alber SM, Di YP, et al.
534 Comprehensive gene expression profiles reveal pathways related to the
535 pathogenesis of chronic obstructive pulmonary disease. Proceedings of the National
536 Academy of Sciences of the United States of America. 2004;101(41):14895-900.
537 Epub 2004/10/08.
- 538 32. Laviola L, Orlando MR, Incalza MA, Caccioppoli C, Melchiorre M, Leonardini
539 A, et al. TNFalpha signals via p66(Shc) to induce E-Selectin, promote leukocyte
540 transmigration and enhance permeability in human endothelial cells. PloS one.
541 2013;8(12):e81930. Epub 2013/12/19.
- 542 33. Schraufstatter IU, Chung J, Burger M. IL-8 activates endothelial cell CXCR1
543 and CXCR2 through Rho and Rac signaling pathways. American journal of
544 physiology Lung cellular and molecular physiology. 2001;280(6):L1094-103. Epub
545 2001/05/15.
- 546 34. Miller A, Lanir N, Shapiro S, Revel M, Honigman S, Kinarty A, et al.
547 Immunoregulatory effects of interferon-beta and interacting cytokines on human
548 vascular endothelial cells. Implications for multiple sclerosis autoimmune diseases.
549 Journal of neuroimmunology. 1996;64(2):151-61. Epub 1996/02/01.
- 550 35. Dimasi D, Sun WY, Bonder CS. Neutrophil interactions with the vascular
551 endothelium. International immunopharmacology. 2013;17(4):1167-75. Epub
552 2013/07/19.

- 553 36. Voisin MB, Nourshargh S. Neutrophil transmigration: emergence of an
554 adhesive cascade within venular walls. *Journal of innate immunity*. 2013;5(4):336-47.
555 Epub 2013/03/08.
- 556 37. Armuzzi A, Lionetti P, Blandizzi C, Caporali R, Chimenti S, Cimino L, et al.
557 anti-TNF agents as therapeutic choice in immune-mediated inflammatory diseases:
558 focus on adalimumab. *International journal of immunopathology and pharmacology*.
559 2014;27(1 Suppl):11-32. Epub 2014/04/30.
- 560 38. Blandizzi C, Gionchetti P, Armuzzi A, Caporali R, Chimenti S, Cimaz R, et al.
561 The role of tumour necrosis factor in the pathogenesis of immune-mediated diseases.
562 *International journal of immunopathology and pharmacology*. 2014;27(1 Suppl):1-10.
563 Epub 2014/04/30.
- 564 39. Howarth PH, Babu KS, Arshad HS, Lau L, Buckley M, McConnell W, et al.
565 Tumour necrosis factor (TNFalpha) as a novel therapeutic target in symptomatic
566 corticosteroid dependent asthma. *Thorax*. 2005;60(12):1012-8. Epub 2005/09/17.
- 567 40. Berry MA, Hargadon B, Shelley M, Parker D, Shaw DE, Green RH, et al.
568 Evidence of a role of tumor necrosis factor alpha in refractory asthma. *The New*
569 *England journal of medicine*. 2006;354(7):697-708. Epub 2006/02/17.
- 570 41. Holgate ST, Noonan M, Chanez P, Busse W, Dupont L, Pavord I, et al.
571 Efficacy and safety of etanercept in moderate-to-severe asthma: a randomised,
572 controlled trial. *The European respiratory journal*. 2011;37(6):1352-9. Epub
573 2010/11/27.

42. Gupta SC, Tyagi AK, Deshmukh-Taskar P, Hinojosa M, Prasad S, Aggarwal BB. Downregulation of tumor necrosis factor and other proinflammatory biomarkers by polyphenols. Archives of biochemistry and biophysics. 2014;559:91-9. Epub 2014/06/20.
43. Woodside DG, Vanderslice P. Cell adhesion antagonists: therapeutic potential in asthma and chronic obstructive pulmonary disease. BioDrugs : clinical immunotherapeutics, biopharmaceuticals and gene therapy. 2008;22(2):85-100. Epub 2008/03/19.
44. Blume C, Swindle EJ, Gilles S, Traidl-Hoffmann C, Davies DE. Low molecular weight components of pollen alter bronchial epithelial barrier functions. Tissue barriers. 2015;3(3):e1062316. Epub 2015/10/10.
45. Unger BL, Ganesan S, Comstock AT, Faris AN, Hershenson MB, Sajjan US. Nod-like receptor X-1 is required for rhinovirus-induced barrier dysfunction in airway epithelial cells. Journal of virology. 2014;88(7):3705-18. Epub 2014/01/17.

Figure Legends

Fig. 1: Design of the microfluidic culture system. A: A photoresist dry film forming the microfluidic channel is laminated onto a support layer on which a holder is fixed. A permeable Transwell® support is inserted and sealed by a V-ring. B: Schematic section of a epithelial-endothelial co-culture under microfluidic culture conditions.

Fig. 2: Enhanced barrier properties in epithelial-endothelial co-cultures. The integrity of the epithelial and endothelial barriers was monitored by measuring the transepithelial (or endothelial) resistance (TER). A: Epithelial cells (EPI) were

cultured on the apical and endothelial cells (ENDO) on the basolateral side of permeable filter supports for up to 6 days (Mean±SEM, n=11-16 independent experiments). B: Comparison of TER measurements on day 3 of epithelial monocultures (clear bar), epithelial-endothelial co-culture in close proximity on filter supports (black bar) and co-cultures with endothelial cells grown on the bottom of the well at a distance to epithelial cells (grey bar) (Mean±SEM; n=7 independent experiments; *: $p \leq 0.05$ compared to EPI (Wilcoxon)). C: Effect of endothelial cell conditioned medium on TER of epithelial cells after 3 days of culture. TER was normalised to the TER of epithelial monocultures (Mean±SEM; n=10 independent experiments; *: $p \leq 0.05$ (Wilcoxon)).

Fig. 3: Epithelial cells change the morphology during co-culture with endothelial cells. Epithelial (EPI) and endothelial cells (ENDO) were co-cultured for 6-8 days (right panels) and the morphology of the epithelial cells compared to epithelial monocultures (left panels) by microscopy. Analysis by fluorescence microscopy was performed using an anti-occludin antibody (green, panels A and B) and an actin filament specific dye (red, panels C and D). A z-projection of the epithelial cell layer is shown. E and F: Orthogonal views of the z-stacks. G and H: Electron scanning microscopy images of epithelial monoculture (G) and epithelial-endothelial co-culture (H). Images are representative of 3 independent experiments.

Fig. 4: Effect of Poly(I:C) on the physical barrier properties. Epithelial (EPI) and endothelial cells (ENDO) were co-cultured for 6 days and subsequently exposed apically with Poly(I:C), a mimic of viral double-stranded RNA. Epithelial and endothelial monocultures were used as controls. A: Time-dependent changes of the ionic permeability measured by transepithelial resistance (TER) after stimulation with 5µg/ml Poly(I:C) (Mean±SEM; n=8 independent experiments). B: Dose-dependent effect of Poly(I:C) on the TER of epithelial monocultures and co-cultures at 24h. The TER at t=24h is normalised to the TER at t=0h (Mean±SEM, n=8 independent experiments; *: $p \leq 0.05$ compared to untreated control (Wilcoxon)). C: Macro-molecular permeability of the barrier after Poly(I:C) stimulation. Mono- or co-cultures

were apically exposed with FITC-dextran after 21h of Poly(I:C) stimulation and the passage of FITC-dextran into the basolateral compartment was calculated by measuring the fluorescence intensity after 3h (Mean \pm SEM, n=5 independent experiments).

Fig. 5: Time-dependent release of mediators after Poly(I:C) stimulation. After 6 days in culture, epithelial monocultures or co-cultures were transferred to the microfluidic culture system and apically stimulated with 5 μ g/ml Poly(I:C). The basolateral flow through was collected in 2h intervals with an automated fraction collector and mediator release analysed by ELISA. A: Basolateral release of TNF- α in response to Poly(I:C). B: Time-dependent release of CX₃CL1 (fractalkine). Mean \pm SEM, n=7-8 independent experiments.

Fig. 6: Anti-TNF- α attenuates the Poly(I:C) induced release of CX₃CL1 (fractalkine) in the co-cultures. Co-cultures under static conditions were pre-incubated for 1h with anti-TNF- α and subsequently stimulated with Poly(I:C) apically. Basolateral release of CX₃CL1 (fractalkine) was analysed after 24h by ELISA. Mean \pm SEM, n=5 independent experiments; *: p \leq 0.05 (one-tailed paired t-test).

Fig. 7: Poly(I:C) induced expression of endothelial adhesion molecules is inhibited by anti-TNF- α treatment in the co-cultures. Co-cultures were pre-treated with anti-TNF- α for 1h cultures and subsequently stimulated with 5 μ g/ml Poly(I:C) apically. Expression of ICAM-1 (left panels) and E-selectin (right panels) was analysed by fluorescence microscopy after 24h. Images are representative of 3 independent experiments.

Acknowledgment

The authors like to thank Anton Page from the Biomedical Imaging Unit, University of Southampton for his support performing the electron scanning microscopy and Wen C Lim and Michael Olding for isolating HUVECs from umbilical cords.

658 This project was supported by the National Centre for the Replacement, Refinement
659 & Reduction of Animals in Research, UK (NC3Rs, Project Code: G1001598/1),
660 Asthma UK (Project Code 10/060) and the Asthma, Allergy and Inflammation
661 Research (AAIR) charity.

662

663 **Competing interests:** No competing interests declared

664

665 **Author contributions**

666 C.B., R.R. and M.H. designed and performed the experiments; M.L. assisted with
667 electron microscopy analysis; E.J.S, H.M., D.E.D., J.E.C. and T.M.M. conceived the
668 study; C.B. and D.E.D analysed the data and prepared the manuscript. All authors
669 contributed to the discussions of the project and reviewed the manuscript.

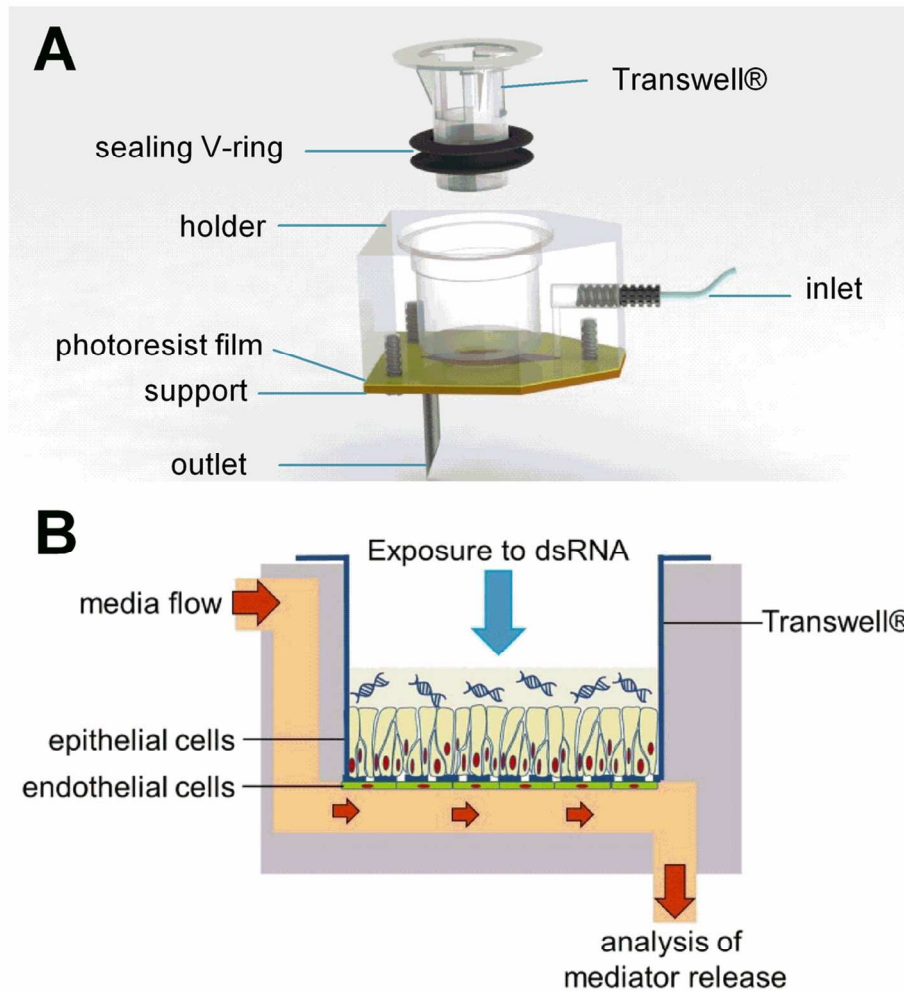


Figure 1: Design of the microfluidic culture system. A: A photoresist dry film forming the microfluidic channel is laminated onto a support layer on which a holder is fixed. A permeable Transwell® support is inserted and sealed by a V-ring. B: Schematic section of an epithelial-endothelial co-culture under microfluidic culture conditions.

Figure 1
111x122mm (300 x 300 DPI)

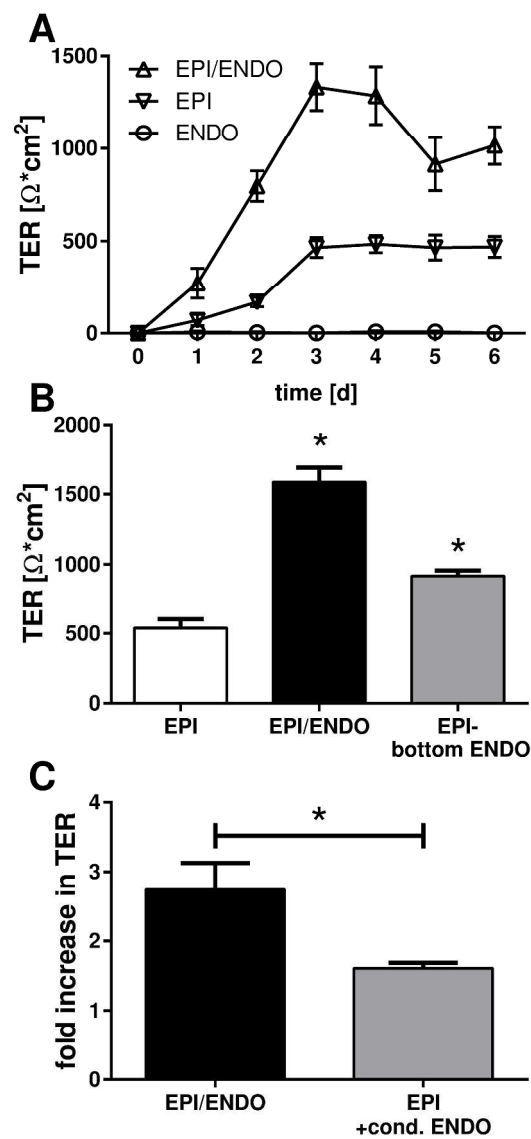


Figure 2: Enhanced barrier properties in epithelial-endothelial co-cultures. The integrity of the epithelial and endothelial barriers was monitored by measuring the transepithelial (or endothelial) resistance (TER). A: Epithelial cells (EPI) were cultured on the apical and endothelial cells (ENDO) on the basolateral side of permeable filter supports for up to 6 days (Mean±SEM, n=11-16 independent experiments). B: Comparison of TER measurements on day 3 of epithelial mono-cultures (clear bar), epithelial-endothelial co-culture in close proximity on filter supports (black bar) and co-cultures with endothelial cells grown on the bottom of the well at a distance to epithelial cells (grey bar) (Mean±SEM; n=7 independent experiments; *: p≤0.05 compared to EPI (Wilcoxon)). C: Effect of endothelial cell conditioned medium on TER of epithelial cells after 3 days of culture. TER was normalised to the TER of epithelial monocultures (Mean±SEM; n=10 independent experiments; *: p≤0.05 (Wilcoxon)).

Figure 2
219x411mm (300 x 300 DPI)

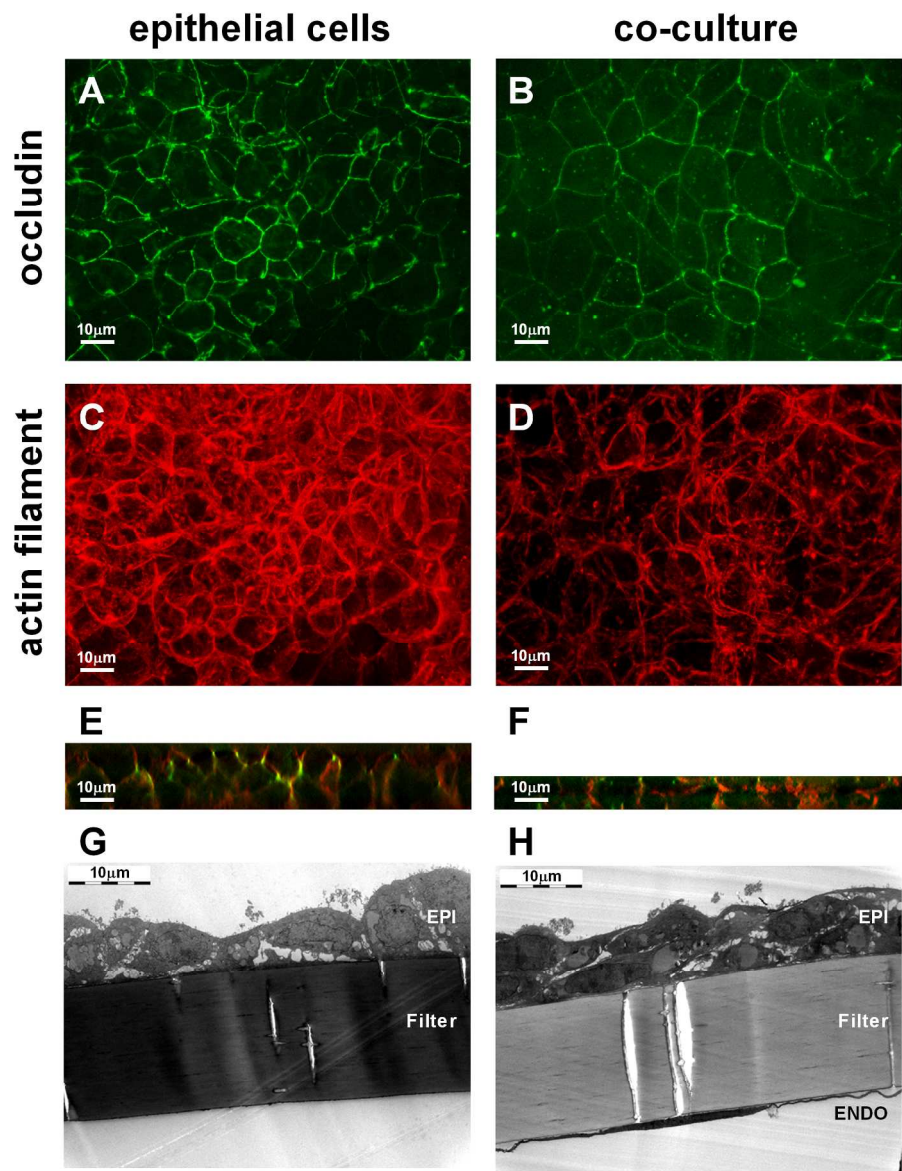


Figure 3: Epithelial cells change the morphology during co-culture with endothelial cells. Epithelial (EPI) and endothelial cells (ENDO) were co-cultured for 6-8 days (right panels) and the morphology of the epithelial cells compared to epithelial monocultures (left panels) by microscopy. Analysis by fluorescence microscopy was performed using an anti-occludin antibody (green, panels A and B) and an actin filament specific dye (red, panels C and D). A z-projection of the epithelial cell layer is shown. E and F: Orthogonal views of the z-stacks. G and H: Electron scanning microscopy images of epithelial monoculture (G) and epithelial-endothelial co-culture (H). Images are representative of 3 independent experiments.

Figure 3
177x228mm (300 x 300 DPI)

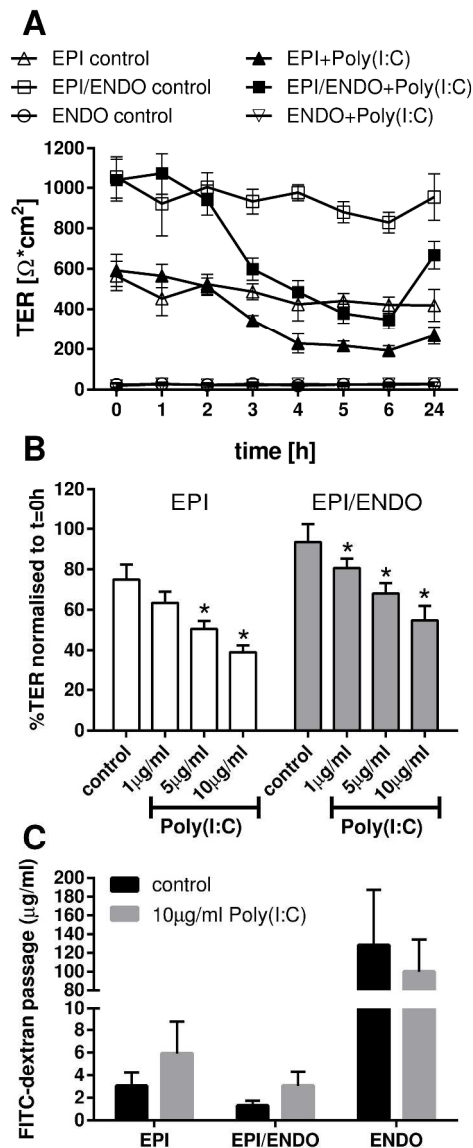


Figure 4: Effect of Poly(I:C) on the physical barrier properties. Epithelial (EPI) and endothelial cells (ENDO) were co-cultured for 6 days and subsequently exposed apically with Poly(I:C), a mimic of viral double-stranded RNA. Epithelial and endothelial monocultures were used as controls. A: Time-dependent changes of the ionic permeability measured by transepithelial resistance (TER) after stimulation with 5 $\mu\text{g/ml}$ Poly(I:C) (Mean \pm SEM; n=8 independent experiments). B: Dose-dependent effect of Poly(I:C) on the TER of epithelial monocultures and co-cultures at 24h. The TER at t=24h is normalised to the TER at t=0h (Mean \pm SEM, n=8 independent experiments; *: p \leq 0.05 compared to untreated control (Wilcoxon)). C: Macro-molecular permeability of the barrier after Poly(I:C) stimulation. Mono- or co-cultures were apically exposed with FITC-dextran after 21h of Poly(I:C) stimulation and the passage of FITC-dextran into the basolateral compartment was calculated by measuring the fluorescence intensity after 3h (Mean \pm SEM, n=5 independent experiments).

Figure 4
251x541mm (300 x 300 DPI)

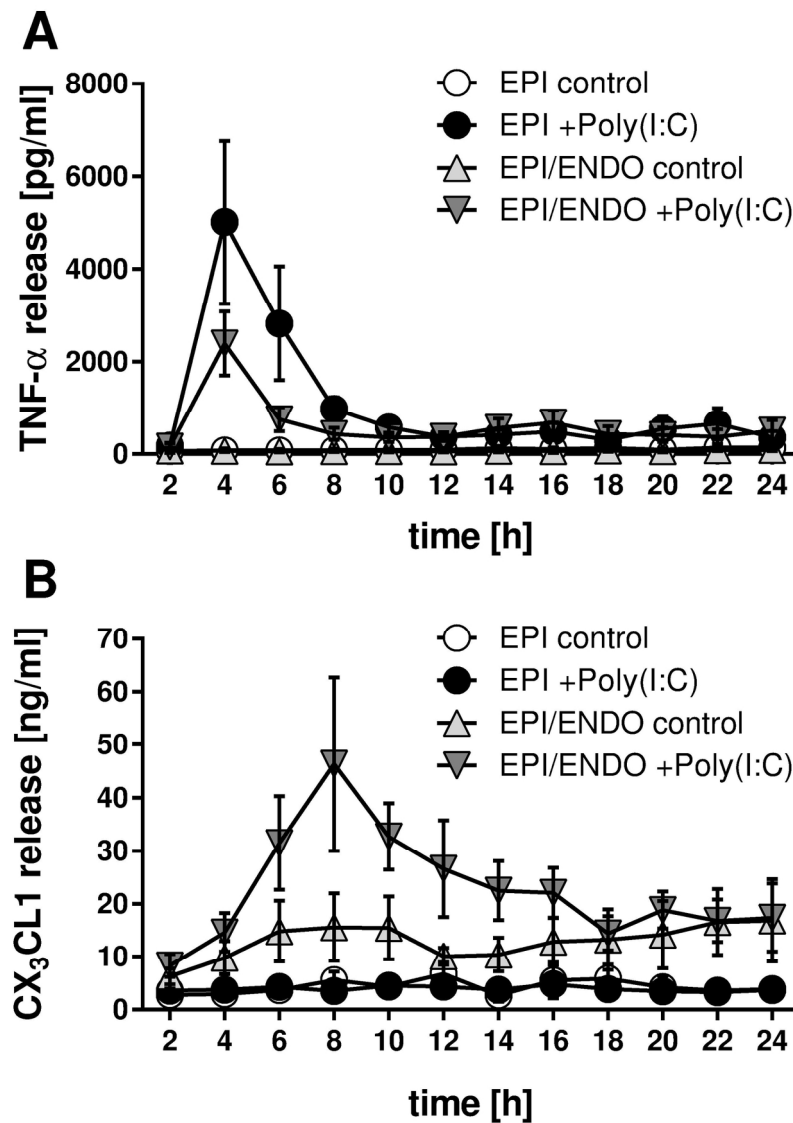


Figure. 5: Time-dependent release of mediators after Poly(I:C) stimulation. After 6 days in culture, epithelial monocultures or co-cultures were transferred to the microfluidic culture system and apically stimulated with 5 μ g/ml Poly(I:C). The basolateral flow through was collected in 2h intervals with an automated fraction collector and mediator release analysed by ELISA. A: Basolateral release of TNF- α in response to Poly(I:C). B: Time-dependent release of CX₃CL1 (fractalkine). Mean \pm SEM, n=7-8 independent experiments.

Figure 5

164x206mm (300 x 300 DPI)

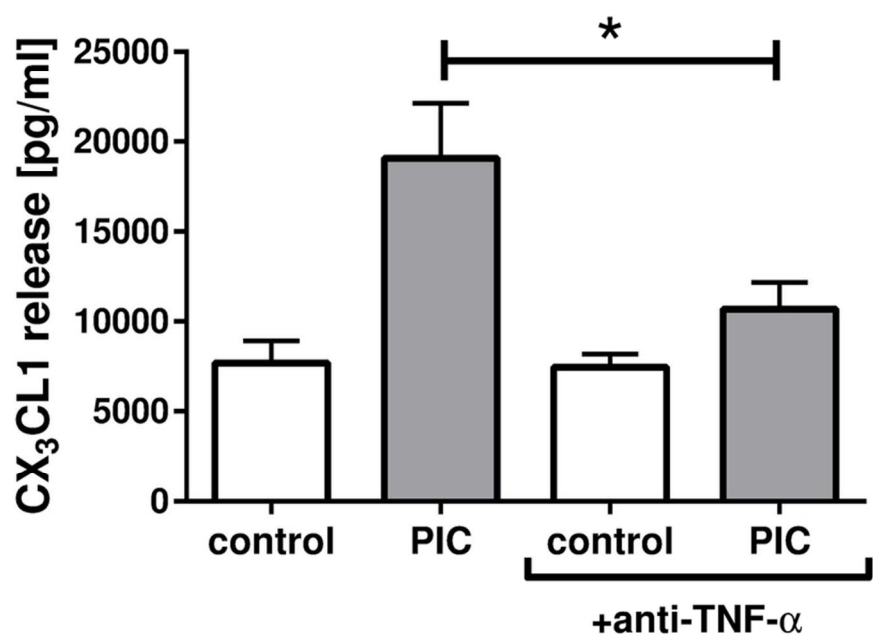


Figure 6: Anti-TNF- α attenuates the Poly(I:C) induced release of CX3CL1 (fractalkine) in the co-cultures. Co-cultures under static conditions were pre-incubated for 1h with anti-TNF- α and subsequently stimulated with Poly(I:C) apically. Basolateral release of CX3CL1 (fractalkine) was analysed after 24h by ELISA. Mean \pm SEM, n=5 independent experiments; *: $p\leq 0.05$ (one-tailed paired t-test).

Figure 6
79x55mm (300 x 300 DPI)

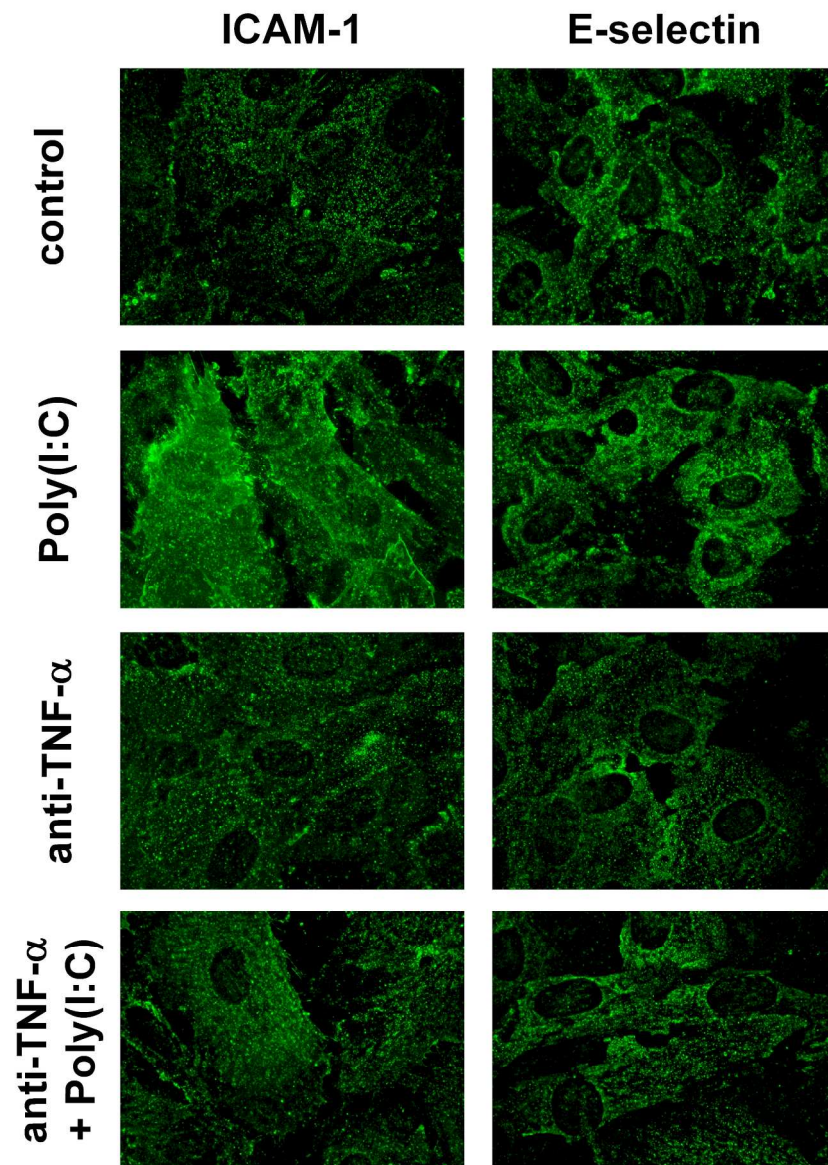


Fig. 7: Poly(I:C) induced expression of endothelial adhesion molecules is inhibited by anti-TNF- α treatment in the co-cultures. Co-cultures were pre-treated with anti-TNF- α for 1h cultures and subsequently stimulated with 5 μ g/ml Poly(I:C) apically. Expression of ICAM-1 (left panels) and E-selectin (right panels) was analysed by fluorescence microscopy after 24h. Images are representative of 3 independent experiments.

Figure 7
208x287mm (300 x 300 DPI)